

A MEMS Frequency Comb Energy Harvester

Teng Zhang and Ashwin A. Seshia, *Fellow, IEEE*

Abstract- This paper reports on the observation of frequency comb phenomena in a mechanically driven piezoelectric MEMS structure configured as a vibration energy harvesting device. By exploring different mechanical driving conditions, both autoparametric resonance and frequency comb response is observed at relatively low drive amplitudes. The harvester response is characterized for both sinusoidal driving and under band-limited noise excitation. Under noisy excitation, the device exhibits frequency comb phenomena spanning multiple octaves. Significant gains in harvested energy are seen when the device is operated in the frequency comb operational mode as opposed to the case of operation in a more traditional resonant regime under the same drive amplitude. The large operational bandwidth and improved power response under noisy excitation offer promise of adapting this approach for practical application.

Index Terms- nonlinear dynamics, mode coupling, internal resonance, frequency comb nonlinear mixing

I. INTRODUCTION

A frequency comb is characterized by several equally spaced and phase-coherent discrete lines in frequency domain. In the optical domain, frequency combs have found numerous applications in metrology and precision time and frequency measurements. In recent years, frequency combs have also been observed in the MEMS domain mediated by nonlinear modal coupling in resonator devices [1-3]. However, most experiments in the MEMS domain have been conducted in the context of electrically driven resonator devices and the observation of frequency combs is reliant on a number of parameters including the nature and strength of the modal coupling, associated damping factors, and driving parameters. In the context of piezoelectric MEMS resonators, there has been limited study of frequency comb phenomena in mechanically driven systems. This letter reports a distinctive frequency comb in a mechanically driven MEMS device. The device design can be adapted for vibration energy harvesting applications and requires a single unidirectional mechanical vibration signal with acceleration as low as 0.07 g (0.69m/s^2) for the onset of frequency comb response. The proposed design is based on two-mode, three-wave mixing arising from nonlinear modal interaction inherent the MEMS device. At sufficiently large base acceleration of a particular form, two distinctive modes are excited simultaneously following energy transfer from the externally driven mode to a second coupled mode via internal resonance. The resulting nonlinear wave mixing results in the emergence of frequency comb response. Remarkably, in our study, we observe that the frequency comb not only exists around the response frequencies corresponding to the normal modes, but also around the different harmonics of the driving signal. In the context of a vibration energy harvesting application, this enables an extended bandwidth of operation.

II. DESIGN

Frequency combs can result from nonlinear mixing of signals comprising different frequencies. Such inherent signal mixing in driven mechanical systems can arise via nonlinear modal coupling [4, 5]. In this work frequency comb phenomena is observed in a MEMS structure describing 1:2 internal resonance [6, 7]. One of the biggest challenges in designing such a MEMS system is the precise definition of key system parameters governing comb response. Factors such as manufacturing tolerances, variations in mechanical properties of the structural films, and environmental effects can influence key system parameters governing comb response.

In this work, the harvester design comprises of a silicon micromachined inner plate attached to a central anchor pedestal and connected to an external outer frame. Fig.1A shows the photo of the packaged MEMS chip. The harvester chip has dimensions of $11\text{ mm} \times 11\text{ mm}$, where the inner plate is separated from the outer frame by two $9\text{ mm} \times 0.1\text{ mm}$ trenches on either side. A central rectangular post with dimensions $1.5\text{ mm} \times 4.5\text{ mm}$ extends from the inner plate and serves as the anchor for the structure as a whole. A total of four electrodes covers the active area in the inner plate with two electrodes each situated on either side of the anchored region. The device stack comprises of a $3\text{ }\mu\text{m}$ AlN piezoelectric layer on a $25\text{ }\mu\text{m}$ single-crystal silicon device layer. The part not covered by electrodes and anchors has an additional $400\text{ }\mu\text{m}$ thick single-crystal silicon substrate layer to provide the proof mass component of the inertial energy harvesting device. Aluminum pad metallization is employed for the top electrode layer, metal interconnect and bondpads. The first three modes are illustrated in Fig. 1 B-D with the first mode corresponding to torsional motion of the outer frame and the third mode corresponding to vertical translation of the outer frame coupled to the bending of the inner plate.

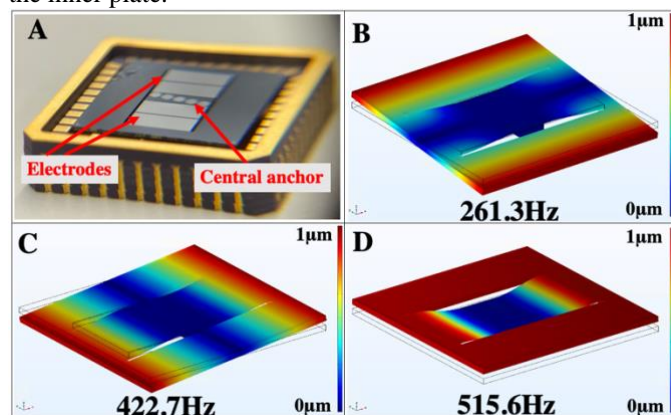


Fig.1 A: Photo of the packaged MEMS energy harvester. B-D: COMSOL simulated results of first three modes at 261.3 Hz, 422.7 Hz and 515.6 Hz respectively. The harvester is anchored by a central rectangular post from the bottom.

Finite Element Analysis of the vibration modes shows that the first three modes of the MEMS harvester are situated at approximately 261.3 Hz, 422.7 Hz and 515.6 Hz respectively. An approximately 1:2 frequency ratio is observed when comparing the natural frequencies for the first and third modes.

III. EXPERIMENTAL CHARACTERIZATION

The harvester is mounted on a shaker, which is driven by a signal derived from an external signal generator whose output is amplified by a power amplifier before feeding it to the shaker. An external analog accelerometer is mounted next to the harvester as a reference to record the base acceleration. At first, the fabricated VEH chip was tested under an open-loop frequency sweep of the shaker excitation conducted at low acceleration levels (< 0.02 g). The measured response confirmed that the resonances of the first three mechanical modes of the representative device occur at 281 Hz, 396 Hz and 565 Hz respectively. Under the right driving conditions, 1:2 internal resonance is observed due to coupling between the first and third modes. The evolution of frequency comb (FC) generation in the designed MEMS harvester is depicted in Figure 2. Four distinct phases can be observed, starting with linear resonant behavior at minimal acceleration as shown in Figure 2A. As acceleration increases, the harvester undergoes Duffing hardening response until a critical base acceleration of 0.05g is reached as depicted in Figure 2B, where the system demonstrates nonlinear hardening behavior with increased bandwidth compared to the linear case. With further increase in the base acceleration, the harvester enters the internal resonance regime characterized by a sudden dip in forward frequency sweep results, as shown in Fig. 2C. The observed sudden dip indicates energy transfer into a coupled mode. Finally, upon exceeding the frequency comb threshold, as seen in Fig. 2D, the system response abruptly transitions to spontaneous oscillations, characteristic of FC behavior. This behavior is consistent with similar observations in other electrically driven resonator systems describing FC response [1-2].

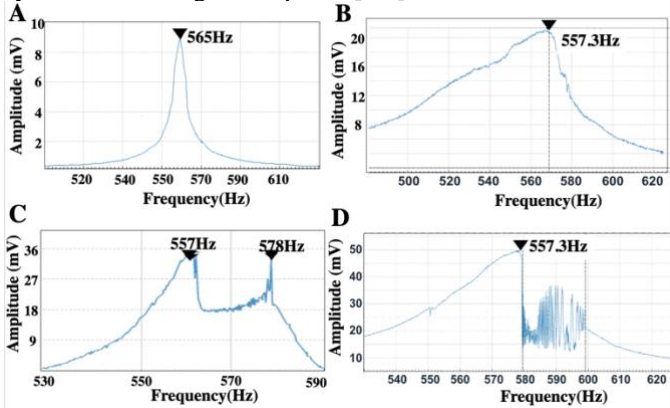


Fig. 2 A: Frequency sweep around the comb mode under low acceleration shows a linear response. B: A frequency sweep under moderate acceleration levels shows evidence of Duffing nonlinearity. C: Increasing the driving acceleration until internal resonance occurs. D: Further increase of the driving levels results in the emergence of the frequency comb.

Aside from the driving level, a second determining factor in inducing frequency comb response is the choice of driving

frequency. The frequency comb arises from signal mixing of three distinctive signals at f_{drive} , f_{comb} , and $f_{coupled}$, where f_{comb} and $f_{coupled}$ are frequencies of frequency comb mode and the coupled mode, which are recognized as the third mode and first mode in this design. The driving signal is offset from the comb mode frequency by a detuning level $\delta_{detuning} = |f_{drive} - f_{comb}|$. As shown in Fig. 3, the detuning factor should be set to be large enough so that the driving signal is distinctive from comb mode and coupled mode signal, yet not too large otherwise the resulting frequency mismatch does not result in efficient excitation of the coupled modes. From the experiment, an optimal range of frequencies for driving signal to trigger the nonlinear signal mixing for frequency comb response is observed and this is marked as the comb regime in Fig. 3B. The lower and higher frequency limits f_{low} and f_{high} for such a regime is proportional to the driving level or acceleration [8]. Under a base acceleration of 0.07g, the frequency comb regime is measured to be $1.3 \text{ Hz} \leq |\delta_{detuning}| \leq 21.2 \text{ Hz}$, and the driving signal within that frequency range could induce three-wave mixing, leading to the emergence of a frequency comb.

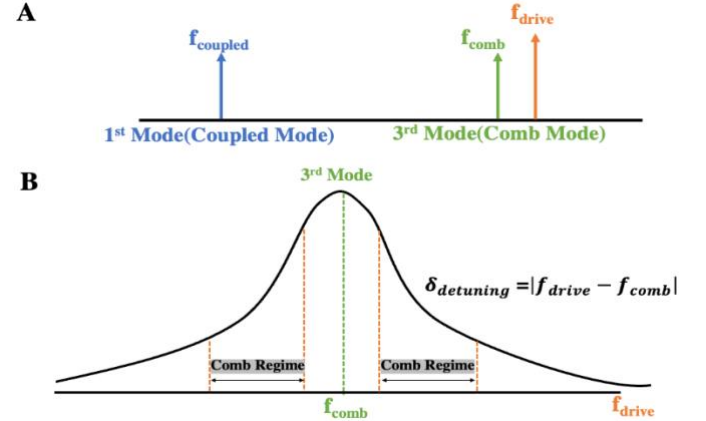


Fig. 3 A: Intermodulation involving three distinct signals from the comb mode, coupled mode, and drive signal. B: Depiction of the comb regime and corresponding detuning level $\delta_{detuning}$.

From Fig. 4A, when directly driving and targeting the third mode as the comb mode with $\delta_{detuning} = 0$ Hz, both the comb mode at 578.4 Hz and the coupled mode at 289.1 Hz are excited. The harvester's electrical output was then recorded across its top and bottom electrodes. In the frequency domain, the electrical output shows a significant amplitude corresponding to the two modes. When slightly moving the driving signal off the 3rd mode (comb mode) with a 10 Hz detuning level and same driving acceleration of 0.07 g, the system response demonstrates emergence of a frequency comb spectrum at the driven mode, coupled mode and resulting harmonics. It is worth noting that the peak at 876.6 Hz is a higher-order harmonic, mirroring the peak at 289.1 Hz with respect to the central peak at 578.4 Hz in the frequency domain. These peaks correspond to triggered higher-order harmonics, indicating non-linear signal mixing between the drive and comb modes. The comb spacing between adjacent comb lines in the spectrum shown in Fig. 4B is equal to the detuning level of 10 Hz. The nominal value of the harvester electrical impedance is measured to be 400000 Ω , and for

energy harvesting experiments, a matched external load resistor is employed for power transfer. When driven with a single-tone signal in the frequency comb mode, a total output power of $14.74 \mu\text{W}$ is measured under 0.07 g acceleration, which is significantly improved compared to direct excitation case of $4.03 \mu\text{W}$ for the non-comb mode at the same acceleration level. For an elevated base acceleration of 0.39 g , the measured output power level was found to increase to 0.22 mW at a detuning level of 6 Hz .

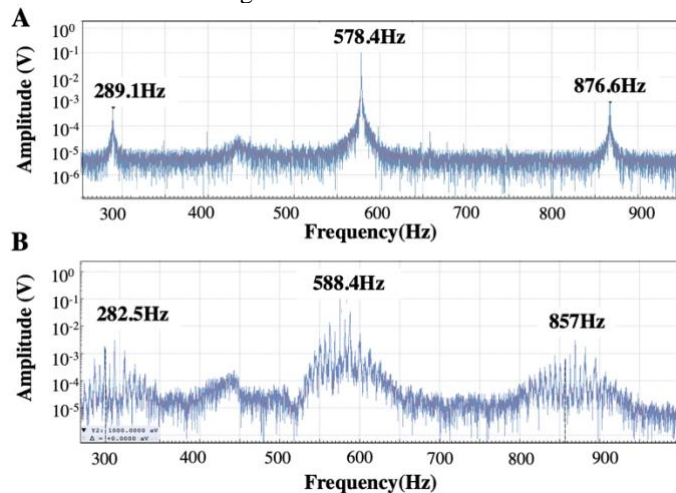


Fig. 4 A: Spectrum indicating internal resonance and mode coupling when driving with a single tone signal at 578.4 Hz . B: Spectrum characterizing frequency combs when driving with a single tone signal at 588.4 Hz and 10 Hz detuning level.

To further characterize the output power performance of the frequency comb harvester, the comb bandwidth is studied as a critical parameter. In the experiment, it is observed that the detuning and the driving levels largely determines the comb spacing and the number of comb fingers which contributes to the total comb width. A far-detuned vibration signal results in a weak mode coupling and requires a high driving acceleration threshold to induce frequency comb response. In return it yields large comb spacing but reduced comb density. On the other hand, a near-detuned signal requires a lower driving threshold, and it generates a comb with high density but narrow spacing. Thus, to achieve optimal comb bandwidth, a balance between comb density and spacing through the detuning and base acceleration levels may be obtained.

A further consideration is the assessment of the device's response when subjected to base vibrations that more closely resemble real-world environments, where vibration signals are inherently noisy and encompass a broad frequency range. In this research, the proposed VEH was tested with band-limited vibration noise to simulate a more real-world vibration environment. The shaker is driven by an electrical signal characteristic of band-limited noise and the electrical output of the harvester is then logged and displayed on an oscilloscope. As shown in Fig. 5A, a random noise signal was generated and filtered through a -20 dB passband filter between 300 Hz and 650 Hz . The measurements were repeated for several trials with the driving signals generated independently each time yielding consistent experimental results. The resulting response shows a broadband frequency comb response in contrast to single tone excited case. With multiple modes and harmonics engaged, the

frequency comb spans most frequencies in the range between 100 Hz and 1.4 kHz . This result also has implications for other applications where frequency combs spanning multiple octaves are of interest.

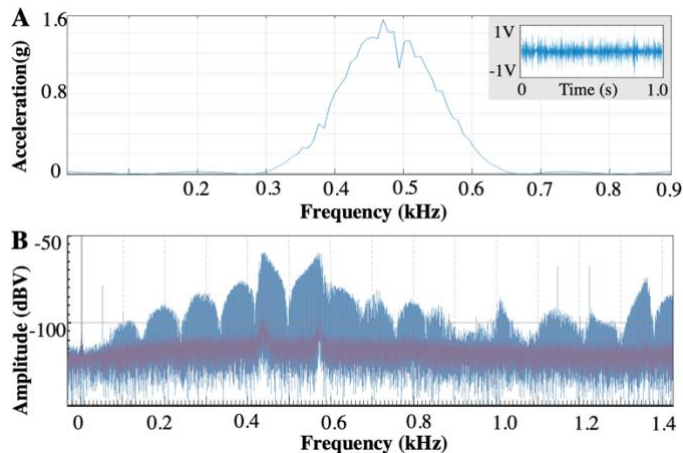


Fig. 5 A: Band-limited noise spectrum (with inset showing the corresponding time-domain) of the electrical signal used to drive the shaker. B: Output spectrum of the frequency comb driven by noise with the response spanning multiple octaves.

IV. SUMMARY

We demonstrate a MEMS vibration energy harvester demonstrating frequency comb behavior under mechanical excitation. Such phenomena can enhance the harvested energy relative to vibration energy harvesters based on linear resonance. We measured an output power of 0.22 mW for a detuned sinusoidal excitation of 0.39 g . Significant improvements are also seen under driving conditions representative of practical environments where the ambient vibration can be noisy. In the experiments, the base acceleration and frequency detuning levels are seen to have an influence on the emergence and evolution of the frequency comb. Future work to develop detailed physical models of the underlying dynamics can enable improvements in performance including engineering the onset of frequency comb phenomena at reduced input acceleration thresholds and allowing for enhanced response bandwidth.

REFERENCES

- [1] A. Ganesan, C. Do, and A. Seshia, "Phononic frequency comb via intrinsic three-wave mixing," *Physical review letters*, vol. 118, no. 3, p. 033903, 2017.
- [2] J. Sun *et al.*, "Generation and Evolution of Phononic Frequency Combs via Coherent Energy Transfer between Mechanical Modes," *Physical Review Applied*, vol. 19, no. 1, p. 014031, 2023.
- [3] L. Bu, E. Arroyo, and A. A. Seshia, "Frequency combs: a new mechanism for mems vibration energy harvesters," in *2021 21st International Conference on Solid-State Sensors, Actuators and Microsystems (Transducers)*, 2021: IEEE, pp. 136-139.
- [4] L. Cao, D. Qi, R. Peng, M. Wang, and P. Schmelcher, "Phononic frequency combs through nonlinear resonances," *Physical review letters*, vol. 112, no. 7, p. 075505, 2014.
- [5] M. Park and A. Ansari, "Formation, evolution, and tuning of frequency combs in microelectromechanical resonators," *Journal of Microelectromechanical Systems*, vol. 28, no. 3, pp. 429-431, 2019.
- [6] A. H. Nayfeh and D. T. Mook, *Nonlinear oscillations*. John Wiley & Sons, 2008.
- [7] A. H. Nayfeh and P. F. Pai, *Linear and nonlinear structural mechanics*. John Wiley & Sons, 2008.
- [8] A. Ganesan, "Phononic frequency combs," University of Cambridge, 2018.